

Chapter 8

Deformation of Polypropylene–EPDM Blends

Reinoud J. Gaymans and Allard van der Wal

University of Twente, P.O. Box 217, 7500 AE Enschede, The Netherlands

Polypropylene-EPDM rubber blends with rubber content varying between 0 - 30 vol. %, were made on a twin screw extruder and their mechanical properties studied. These included the measurement of the notched Izod fracture energy and the notched tensile behavior as function of strain rate ($0.003 - 300 \text{ s}^{-1}$) and also as a function of temperature ($-40^\circ - 140^\circ\text{C}$). During high speed testing, the deformation zone of the sample, warm up, and temperature development were followed using an infrared camera. The structure of the deformation zone was studied by scanning electron microscopy.

The blends were found to exhibit a sharp brittle-ductile transition and have high fracture energies in the ductile region. By increasing the rubber content, the brittle ductile transition shifted strongly towards the lower temperatures. The deformation process changed with temperature and test speed, the test speed effect possibly being due to a strong adiabatic heating in the fracture plane and therefore a thermal blunting mechanism is proposed.

Introduction

Polypropylene (PP) is a semi-ductile material which, when unnotched, has a high impact strength, and when notched, fractures in a brittle manner. With increasing temperature, the material becomes ductile at the brittle-ductile transition. For PP, the brittle-ductile transition temperatures (T_{bd}) on notched samples and measured in Izod are well above room temperature (T). The T_{bd} can be lowered by the incorporation of a rubbery dispersed phase; the rubber can be blended in by using an extrusion compounding process, or can be polymerized in. Although incorporation by polymerization is the usual industrial practice(2), the extrusion process is more flexible in studying the behavior of the blend as a function of morphology. PP is usually modified with EPR and EPDM rubber but can also be toughened by using SBS, SEBS, polybutadiene and polyisoprene(3-13).

With rubber modification, the modulus and the yield strength are reduced, the notched Izod energy is increased, and a considerable shift in the brittle-ductile transition temperature is observed. The function of the rubber is to cavitate and thereby change the stress state of the matrix in the vicinity of the cavity (14-19). An additional effect of cavitated particles concentration is a stress field overlap of neighboring cavitated particles(17,18,20,21). As a result of the cavitation, the plane strain condition ahead of a notch is gradually changed to a plane stress state and shear yielding of the matrix becomes more likely to occur. Shear yielding and crazing are competitive processes, the one with the lowest stress occurring. At the brittle-ductile transition, the yield stress crosses over with the craze stress. This transition state is sensitive to changes in material parameters and test conditions.

The notched Izod impact method is often used for studying the impact behavior of engineering plastics. With an increasing rubber concentration, the notched Izod fracture energies of PP increase (Figure 1)(12).

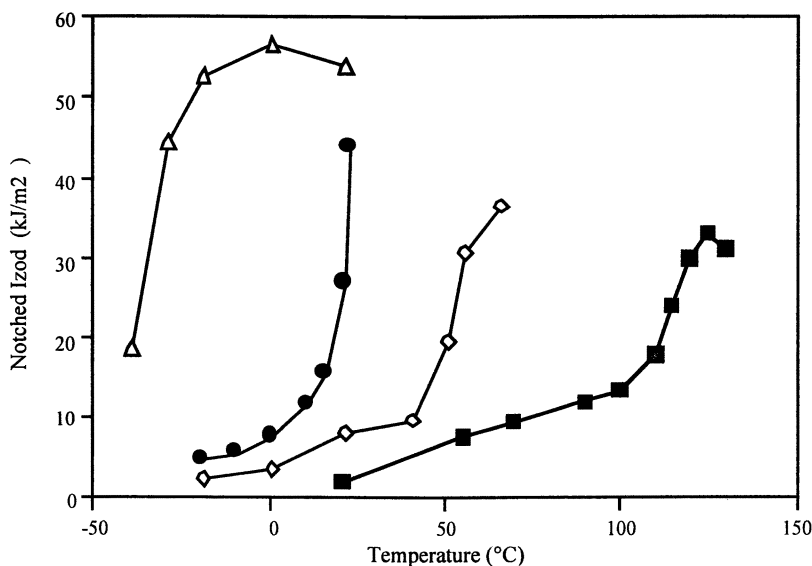


Figure 1. Notched Izod as function of temperature of PP/EPDM with varying rubber content (vol. %): ■, 0%; ◇, 15%; ●, 20%; △, 30%. Reproduced with permission from reference 12.

At low temperatures (-40°C), the samples fracture in a brittle manner and the fracture energy increases with increasing rubber content. At high temperatures, the samples deform ductile and are no longer fully broken. In addition, the T_{bd} transition is also shifted towards a lower temperature with an increasing rubber content. Samples that exhibit brittle fracture have: a relative low fracture energy (1-20 kJ/m²), stress whitening in the notch, a thin stress whitened layer adjacent to the fracture plane and a high fracture speed (> 200 m/s). Samples that fracture in a ductile manner have: a much higher fracture energy, a stress whitened zone adjacent

to the fracture plane (1-2 mm thick) and a low fracture speed (< 50 m/s). The matrix parameters have a direct effect on the impact properties of the blend. By increasing the molecular weight and decreasing the crystallinity of PP, the T_{bd} of the blend is decreased (11).

The morphology of the blend and in particular the rubber particle size, has an appreciable effect on the notched Izod behavior(22). Decreasing the rubber particle size shifts the T_{db} to a lower temperature, this effect is similar to that observed in the polyamide system. The function of the rubber particles is to cavitate; however, the cavitated particles should not become initiation sites for the fracture process. Therefore, the particles must be small enough such that they do not grow to a size where they are able to initiate a crack. It is expected that large particles form large cavities and thus are more likely to initiate fracture.

Ductile fracturing blends exhibit extensive plastic deformation. As most of the mechanical energy is dissipated as heat, a marked temperature increase takes place in the notch area(13). If the plastic deformation takes place under adiabatic conditions (at high strain rates), an even stronger temperature rise can be expected.

These ductile materials are generally studied using the notched Izod method. An additional, and very useful method is the single edged notch tensile (SENT) test (12). This instrumental method provides information on the fracture stress, strain development before crack initiation and strain development following crack initiation. In the notch, plastic deformation can take place prior to a crack being initiated. At the moment of crack initiation, stresses are likely to be at their maximum and at this point a considerable amount of elastic energy is stored in the sample. If this elastic energy is sufficient to lead to fracture of the sample, then the crack proceeds fast and the fracture type is brittle. If the elastic energy in the sample is insufficient to fracture the sample, more energy has to be supplied. The fracture speed is therefore much lower and the fracture proceeds in a ductile manner.

In this paper we have studied the influence of strain rate on the fracture behavior of PP-EPDM blends using the SENT test method.

Experimental

The materials used encompass a polypropylene homopolymer (Vestolen P7000, Vestolen GmbH) with an MFI of 2.4 (230 °C, 21.6 N) and an EPDM rubber (Keltan 820, DSM). A series of blends of varying rubber content were prepared by diluting a PP-EPDM (60/40 vol. %) extrusion master blend and rectangular bars and dumbbell-shaped specimens prepared by injection molding. The blending and injection molding processes have previously been described in detail (12).

The SENT tests were carried out on notched bars using a Schenck servo-hydraulic tensile machine. The injection-molded bars (ISO 180/1, 74x10x4 mm) had a milled, single-edge, 45 ° V-shaped notch (depth 2 mm, tip radius 0.25 mm). The clamp length of the samples was 45 mm. The Schenck tensile apparatus is specifically designed for high speed testing, in that the studied clamp speeds range from 10^{-5} to 10 m/s. At high test speeds, a pick-up unit was used, thus allowing the piston to reach the desired test speed before specimen loading. To minimize inertia effects, all moving parts were made of titanium. Force and piston displacement were recorded using a transient recorder (sample rate 2 MHz) and following test completion, all results were downloaded to a computer. All measurement were carried out in five fold.

The temperature rise during fracture was measured by an infrared camera (IQ 812 system from Flir Systems) (13), the signal from which was sent to a computer.

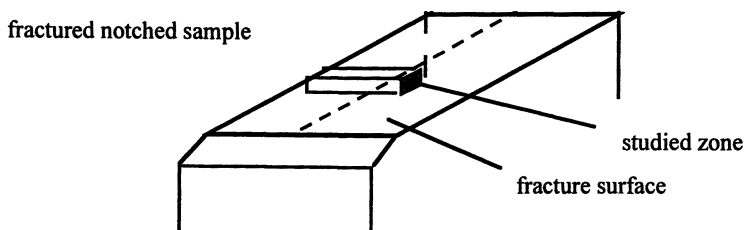


Figure 2. Sample position

The mechanism of deformation of the fracture zone was studied by post-mortem using scanning electron microscopy (SEM), the sample position studied is shown in Figure 2.

The area of interest is perpendicular to the fracture surface and runs parallel to the crack growth direction. Samples were taken from the specimens using a fresh razor blade and then smoothed down on a polishing machine to avoid deformation during the trimming procedure. The finishing preparation was carried out by sectioning at $-100\text{ }^{\circ}\text{C}$ with a diamond knife and the final surface sputter-coated with a gold layer before analysis and studied using a Hitachi S-800 field emission SEM.

Results and Discussion

The studied PP-EPDM blends were prepared by extrusion blending, the particle sizes obtained are shown in Table 1.

Table 1. Particle size in PP-EPDM extrusion blends

Rubber Content	5%	10%	20%	30%	40%
Dw (μm)	0.50	0.67	0.69	0.86	0.92

The particle size increases with increasing rubber content, however such a particle size difference is known to have only a small effect on the brittle-ductile transition(22). The tensile and physical properties of the blends used have previously been reported(12).

Fracture behavior as a function of test speed was studied by using a single-edge notched tensile (SENT) test. The influence of test speed was examined by varying the clamp speed from 10^5 to 10 m/s. With these test speeds, a clamp length of 45 mm and a notch, the observed apparent strain rates in the elastic loading part are in the range $0.000275 - 275\text{ s}^{-1}$.

The fracture process can be divided into two stages, these being 'initiation' and 'crack propagation'. During 'initiation', the stress increases at the site of the notch tip, but is still too low to allow crack propagation. Crack propagation begins at or past the stress maximum in the stress displacement curve. We found that PP deformed in this SENT test at room temperature, remained brittle over the whole strain rate range.

The fracture energy at 27.5 s^{-1} (1 m/s) was studied as function of test temperature at different EPDM contents. When using the SENT test, the samples were always fully broken, the fracture energies being reliable up to high temperatures. S-type curves were obtained and with increasing rubber content these S-type curves are shifted to lower temperatures (Figure 3).

At low temperatures the samples fractured in a brittle manner having a low fracture energy. At high temperatures they fractured in a ductile manner following a sharp brittle-ductile transition. The fracture energies in SENT were considerably higher than those obtained in Izod. In tensile loading (SENT), more material was plastically deformed and the stress-whitened zone was thicker, particularly at the end of the fracture path. With an increasing rubber content, the S-curves were shifted to lower temperatures. In the brittle region (-30°C), fracture energies increased with increasing rubber content (Figure 4).

At -30°C the fracture is in all these cases brittle and this increase in fracture energy is due solely to the increased deformation in the notch. As with increasing rubber content deformation in the notch area becomes stronger and the fracture energy increases. In this brittle region, the fracture energies as measured in SENT are comparable to the fracture energies as measured in notched Izod. At high temperatures (120°C) the fracture is in all cases ductile and the fracture energies decreased with increasing rubber content. The function of rubber is to cavitate and change thereby the stress state. The high fracture energy comes from the plastic deformation of the matrix. This plastic deformation is enabled by the rubber particles. Once a material fractures ductile at a particular temperature than more rubber does not further enhance the fracture energy it even decreases the fracture energy as the matrix content is decreased with increasing rubber content. Surprisingly, the 1% and 5% blends have higher fracture energies than neat PP.

The ductile region (past the T_{bd}) the fracture energy decreases with increasing temperature (Figure 3) is due to the corresponding strong decrease in yield strength with temperature.

Once a material fractures in a ductile manner a further lowering of the yield strength does not so much enhance the fracture strain but lowers the fracture energy. The brittle-ductile transition temperature was found to decrease with increasing rubber content (Figure 5). This decrease is similar to that observed in the notched Izod test; therefore the SENT test at 1 m/s is comparable to the notched Izod. T_{bd} decreased steadily with increasing rubber content. Therefore it appears that a small percentage of rubber is insufficient to relieve all of the volume strain. The glass transition of PP (at 5°C) had little effect on this T_{bd} shift. Below its T_g , PP has a more brittle behavior but this is apparently balanced by a more effective toughening by the rubber. Below its T_g , the PP has a lower Poisson-ratio which makes the material more susceptible to crazing, however, if the matrix has a low Poisson-ratio the rubber cavitation takes also place more easily.

The SENT studies at different strain rates were carried out in two parts. Firstly, a fixed rubber concentration was used (10% EPDM) and the temperature varied, secondly, the rubber concentration was varied whilst the temperature was held constant at room temperature.

The stress displacement curves as obtained by SENT on a 10 vol. % blend at low and high strain rates are shown (Figure 6).

At a strain rate of 27.5 s^{-1} , the blends fractured in a brittle manner at 0° and 40°C

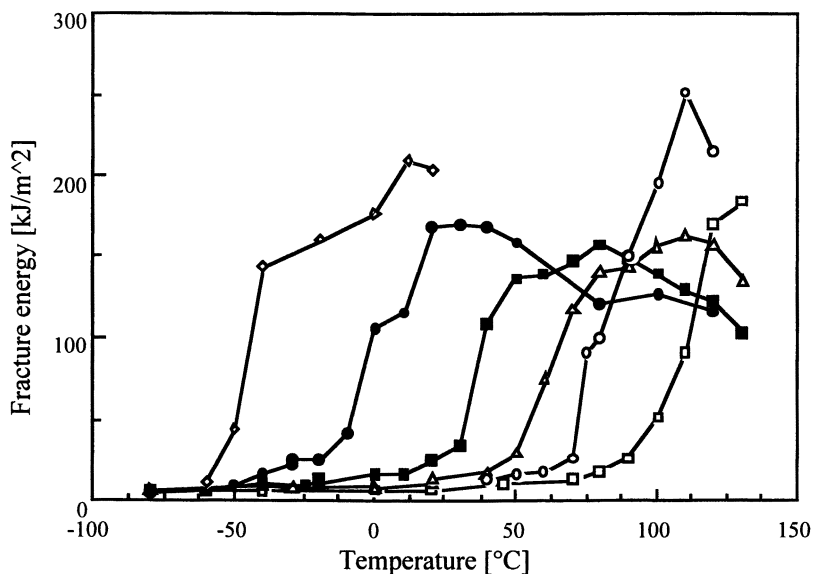


Figure 3. SENT fracture energies as function of temperature measured at 27.5 s^{-1} (1m/s) of PP/EPDM with varying rubber content (Vol. %): \square , 0; \circ , 5; \triangle , 10; \blacksquare , 20, \bullet , 30; \diamond , 40. Reproduced with permission from reference 12.

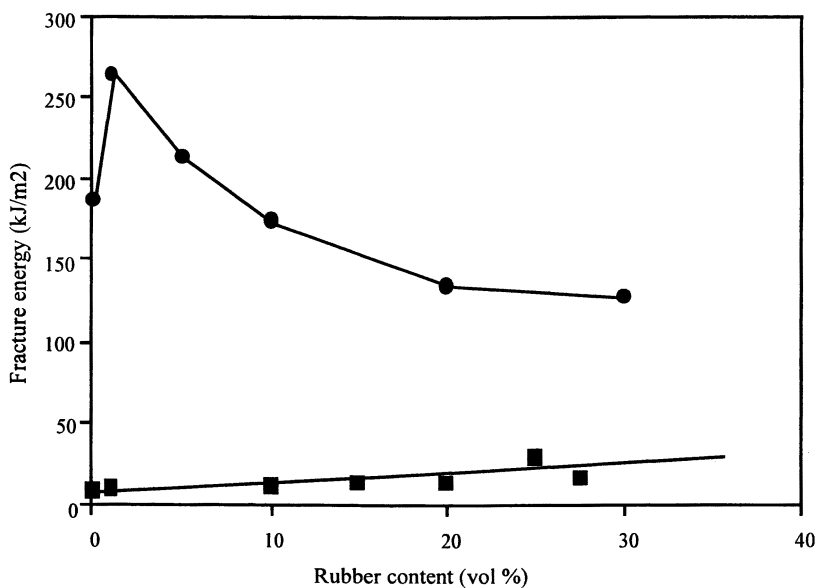


Figure 4. SENT fracture energies as function of rubber content measured at 27.5 s^{-1} (1m/s) and at different temperatures: \blacksquare , -30°C ; \bullet , 120°C .

and in a ductile manner above 60°C. The fracture stress decreased strongly with increasing temperature. At temperatures of 60°C and higher, considerable yielding occurred in the notch and during fracture. At a strain rate of 0.0275 s⁻¹, the samples became ductile at 20°C and behaved in a fully ductile manner at 50°C. In this 20°-50°C temperature range, the fracture energy in the propagation region is due to deformation with shear lips. The T_{bd} for the 0.0275 s⁻¹ strain rates was measured as a function of the rubber content (Figure 5). At this strain rate, the T_{bd} decreased with increasing rubber content, such that the T_{bd} curve as a function of the rubber content was 30°C lower than that in the 27.5 s⁻¹ SENT results. The more brittle behavior at higher strain rates is as expected.

The stress displacement curves obtained by the SENT test for the 30 Vol. % blend at varying test speeds are shown in Figure 7.

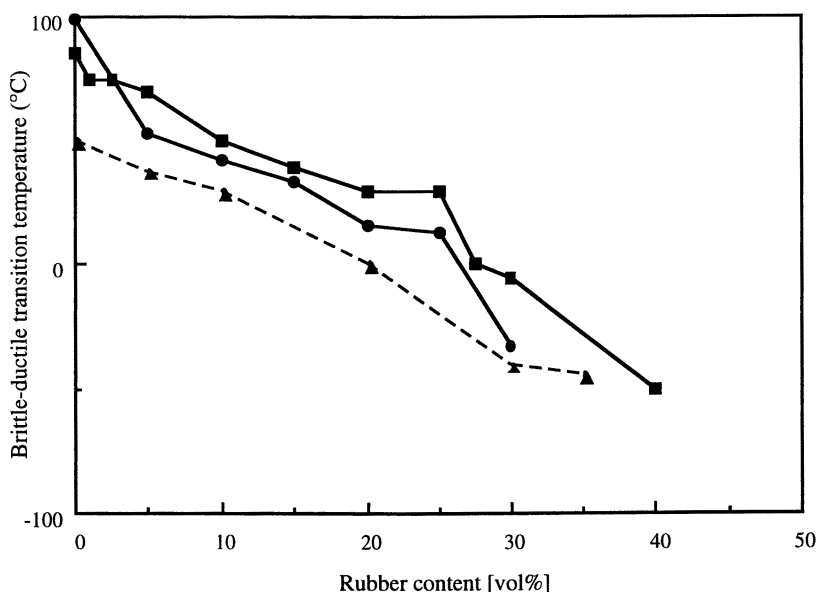


Figure 5. The brittle-ductile transition temperature as function of rubber content: ●, Izod; ■, SENT 27.5 s⁻¹ (1m/s); ▲, SENT 0.0275 s⁻¹ (1 mm/s). Reproduced with permission from reference 12.

The maximum stress of this 30% blend increased with increasing strain rate and considerable plastic deformation was found to take place during crack propagation. Throughout the entire speed range used in the test, this 30% blend fractured in a ductile manner.

For polypropylene and the 30% blend, the maximum stress as function of test speed is shown in Figure 8.

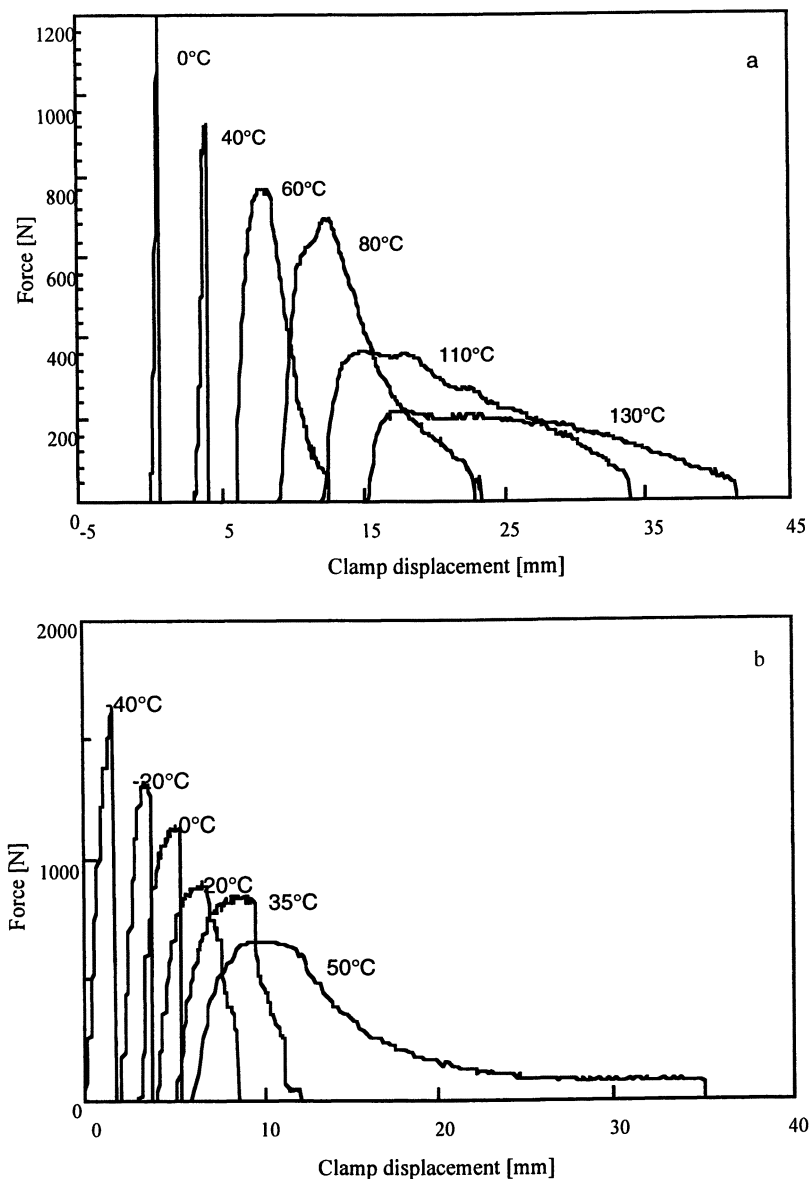


Figure 6. SENT stress displacement curves of PP/EPDM (90/10) measured at different temperatures: a, 27.5 s^{-1} ; b, 0.0275 s^{-1} .

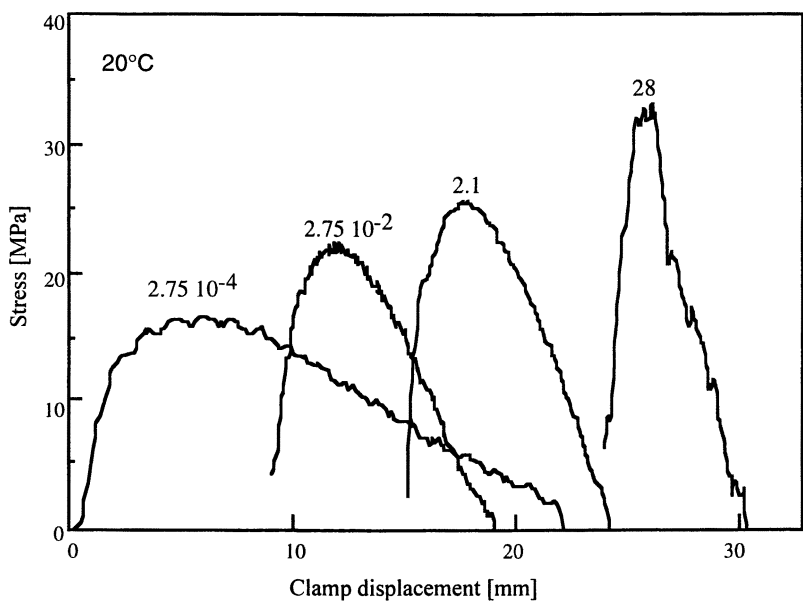


Figure 7. SENT stress displacement curves of PP/EPDM (70/30) measured at different strain rates. Reproduced with permission from reference 13.

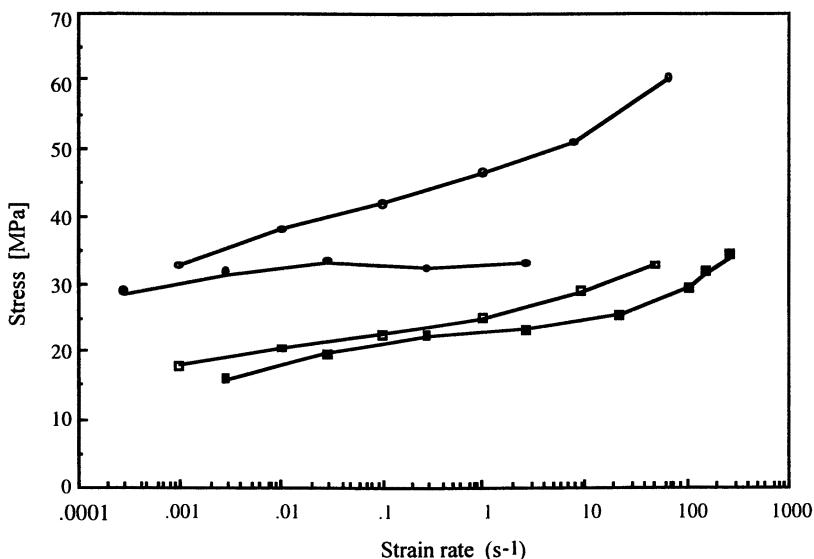


Figure 8. The yield stress in tensile and the maximum stress in SENT as function of strain rate: ○, PP tensile; □, PP SENT; ●, PP/EPDM (70/30) tensile; ■, PP/EPDM (70/30) SENT. Reproduced with permission from reference 13.

For comparison the measured yield stresses for unnotched specimens are also given. At a low strain rate (10^{-3} s^{-1}), PP has a maximum stress that almost equals the yield stress. This suggests that the whole cross section ahead of the notch sustained a yield stress and therefore that the notch must have been blunted. At intermediate test speeds, the maximum stress of the PP curve dropped to a level well below the yield stress, therefore crack propagation started before the entire cross section was bearing a yield stress. If the material fractured before any yielding in the notch had taken place, then it would be expected that there would be a strong decrease in the fracture stress. This was not observed in PP at 20°C or even -40°C

at the strain rates tested. Over almost the whole strain rate region, the 30% blend has a stress that equals the yield stress. At very high strain rates, a strong increase in stress is observed, a similar increase can be seen in the unnotched tensile results. This increase seems to be typical for materials that exhibit a strong plastic deformation in the notch.

The initiation energy (IE) was found to be high at low test speeds and subsequently decrease with increasing test speed (Figure 9a). At very high test speeds, the IE appears to stabilize or even increase. The blends tested exhibited a strong plastic deformation before the initiation of a crack over the entire speed range used. The amount of plastic deformation in the notch before crack initiation was found to decrease with an increased strain rate, however at the higher strain rates, stabilization seemed to occur. This stabilization in the deformation in the notch suggests an enhanced notch blunting effect. Therefore, the amount of plastic deformation in the notch has an effect on the stress concentration in the notch.

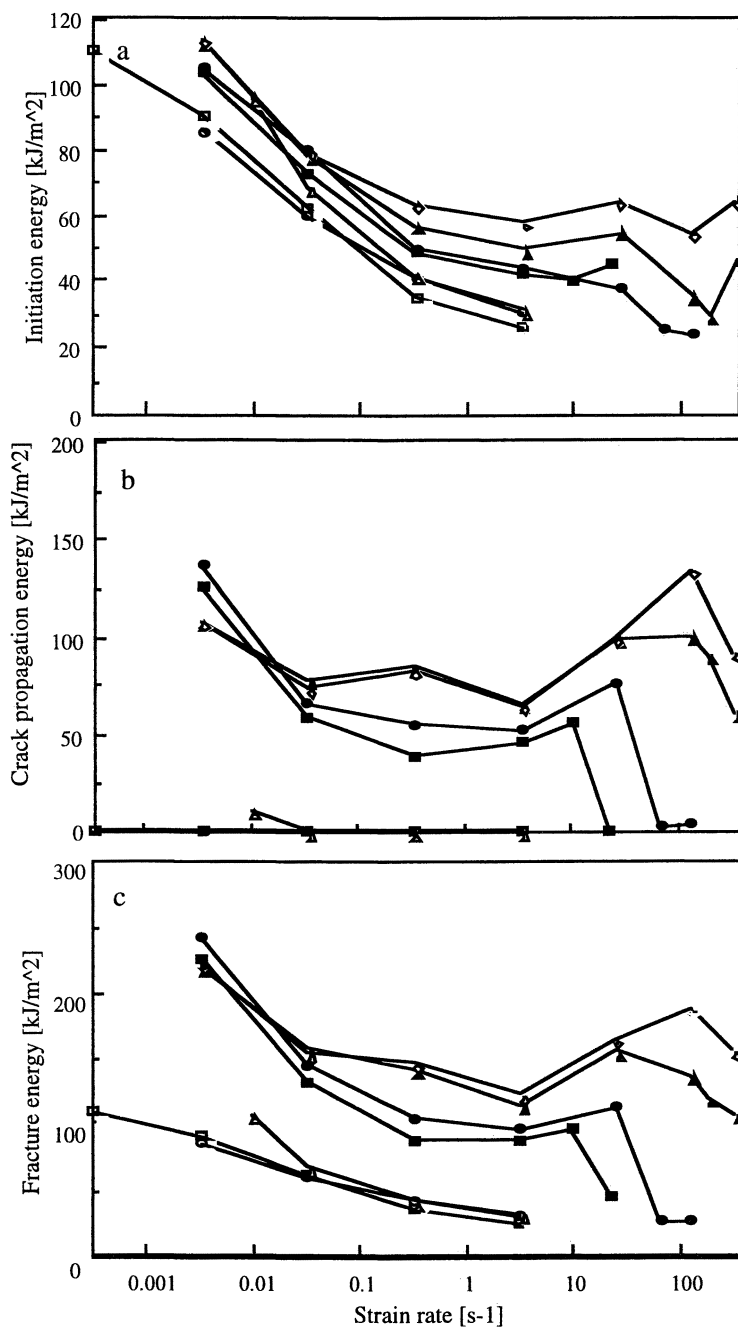


Figure 9. SENT fracture energies as function of strain rate at different EPDM contents (vol%): \square , 0; \circ , 1; \triangle , 5; \blacksquare , 15; \bullet , 20; \blacktriangle , 30; \diamond , 40. Reproduced with permission from reference 13.

The crack propagation energy (CPE) (Figure 9b) curves are complex. At low strain rates, the CPE decreased with increasing strain rate. This was as expected as by increasing the strain rate, the fracture strain decreases. Surprisingly, at intermediate strain rates, the CPE is increased with increasing strain rate. At very high strain rates, it decreases again. The results suggest that at low strain rates with increasing test speeds, the materials turn brittle. However, in all samples, at intermediate strain rates ($0.2 - 2 \text{ s}^{-1}$) this trend is reversed, such that the materials become less brittle. At even higher strain rates, the materials again turned brittle. It seems as if the at high test speeds the fracture process proceeds differently from at low speeds and thereby shifting the trend of decreasing fracture energies with increasing strain rates to higher strain rates. This change at high strain rates is probably the result of an adiabatic plastic deformation accompanied by a strong warming of the sample. A similarly complex behavior of the CPE with strain rate was found in rubber modified nylon, this has been explained as a thermal blunting effect (23). The rubber content had a strong influence on when the blends started to behave in a brittle manner. The higher the rubber content, the higher the strain rate at which the blends turned brittle. The turning ductile at $0.2 - 2 \text{ s}^{-1}$ suggests that at this strain rate, the deformation process undergoes a change.

The total fracture energy (Figure 9c) also exhibits a complex behavior as a function of strain rate. The fracture energy is almost equally dependent on the initiation and the propagation parts of the deformation process. Over the whole strain rate range at this temperature, the fracture energy strongly increased with an increasing rubber concentration. This is due to the fact that neat PP fractures in a brittle manner over the whole strain rate range whilst the 30 % blend is fully ductile over the same range. The other blends exhibit behaviors in-between those of the neat PP and the 30 % blend.

In the blends, plastic deformation clearly takes place in the notch and the process proceeds by ductile fracture during crack propagation. With this strong plastic deformation, a considerable temperature rise can be expected at high test rates. The temperature increase during SENT was studied by using an infrared camera (22). The spatial resolution of the camera is $130 \mu\text{m}$ whilst the strongest deformation can be observed in a $50 \mu\text{m}$ thick layer adjacent to the fracture surface. A typical pattern is shown in Figure 10, the highest temperatures being recorded just ahead of the notch. The maximum wall temperature increased with an increasing strain rate to 90°C at 10m/s . The poor spatial resolution of the infrared camera does not allow the study of the very thin ($50\mu\text{m}$) layer adjacent to the fracture plane, this is the region where the strongest plastic deformation is expected.

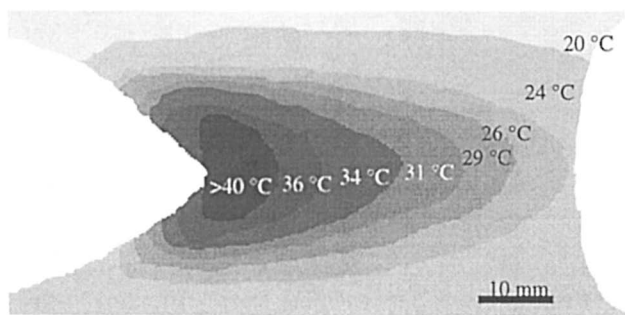


Figure 10. Temperature profile of PP/EPDM (70/30) sample deformed at 0.027 s^{-1} . Reproduced with permission from reference 13.

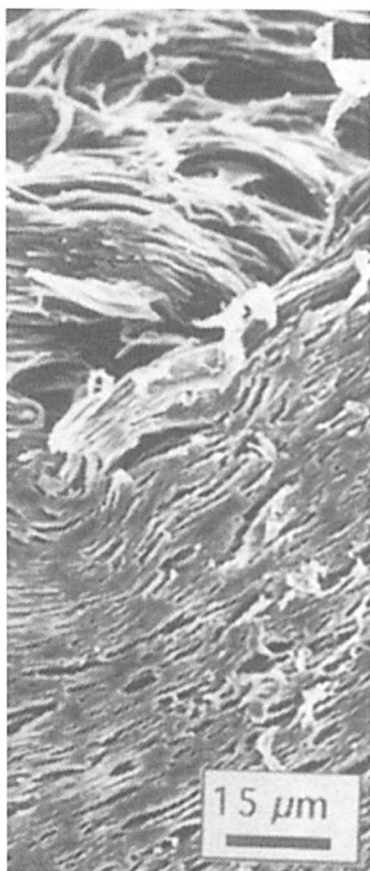
To study the asymmetric deformation process in fractured notched samples, SEM micrographs were made of the fracture zone next to the fracture surface in the middle of the samples. We examined the effect of strain rate on the structure of the fracture zone in a 30 vol. % blend that fractured in a ductile manner (Figure 11).

At low strain rates (0.0275 s^{-1}), on a fracture sample taken from an area adjacent to the fracture surface, strongly elongated cavities could be seen. For cavities at the fracture surface the length/width ratio was 15, thus suggesting a draw ratio for PP of 15. On increasing the samples distance from the fracture surface, the cavities become more rounded. At higher strain rates ($\geq 0.2 \text{ s}^{-1}$), the deformation of the cavities appears to be less than that seen at low strain rates, in that there are no longer any cavities present in the layer adjacent to the fracture surface. In the region just ahead of a crack, a layer without cavities can also be seen. This suggests that in PP-EPDM blends, the elongated cavities disappear at this high strain rate. The cavities seem to have relaxed in the region next to the fracture plane. This may be due to the temperature increase at these high strain rates. Up to approximately 0.275 s^{-1} , the cigar-shaped voids extend to the fracture surface, the thickness of the strongly deformed layer being about $25 \mu\text{m}$. The appearance of the relaxation layer at high test speeds is also observed in nylon 6-rubber blends(23,24). In these blends, the thickness of the relaxation layer was found to be $3\text{-}5 \mu\text{m}$. The appearance of a relaxation layer in polypropylene-EPDM blends at high strain rates and coincides with the CPE increase with the strain rate (Figure 9c).

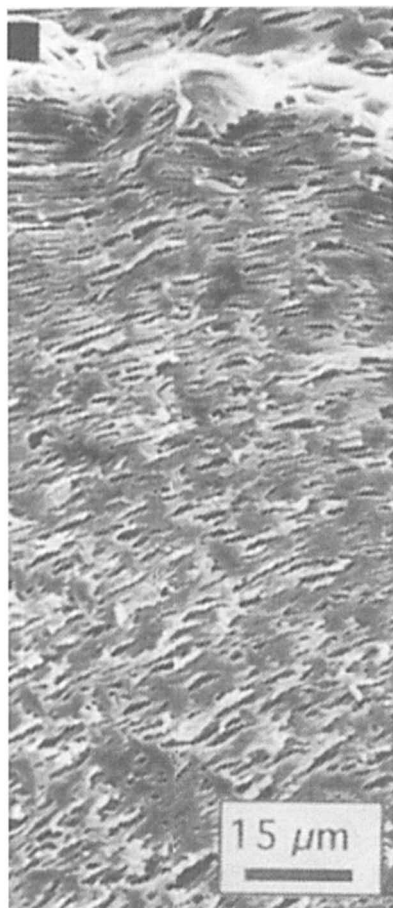
Conclusions

By using the instrumented SENT method, considerable insight into the deformation behavior of PP-rubber blends can be obtained. Notch deformation of PP-EPDM blends, as a function of strain rate is complex. At low strain rates, the crack propagation energy (CPE) was found to rapidly decrease with increasing strain rate. However, at intermediate strain rates ($> 0.2 \text{ s}^{-1}$), the CPE increased with increasing test speed. At these strain rates, the structure of the deformation zone (of the 30% blend) adjacent to the fracture surface changes and the samples exhibit a layer that must have been relaxed. This suggests that during plastic deformation at high strain rates a highly elastic material is present ahead of the notch and that this layer may blunt the notch. This is termed a thermal blunting process.

Thus two observed processes occur. At low strain rates, a fracture process accompanied by strong plastic deformation occurs both during initiation and as propagation proceeds. At high strain rates, a plastic deformation process occurs where there is formation of an elastic layer ahead of the notch front. This thermal blunting process that is taking place at high strain rates considerably enhances the toughness of the blend, if this process did not occur, these blends could well be brittle at the strain rates used.

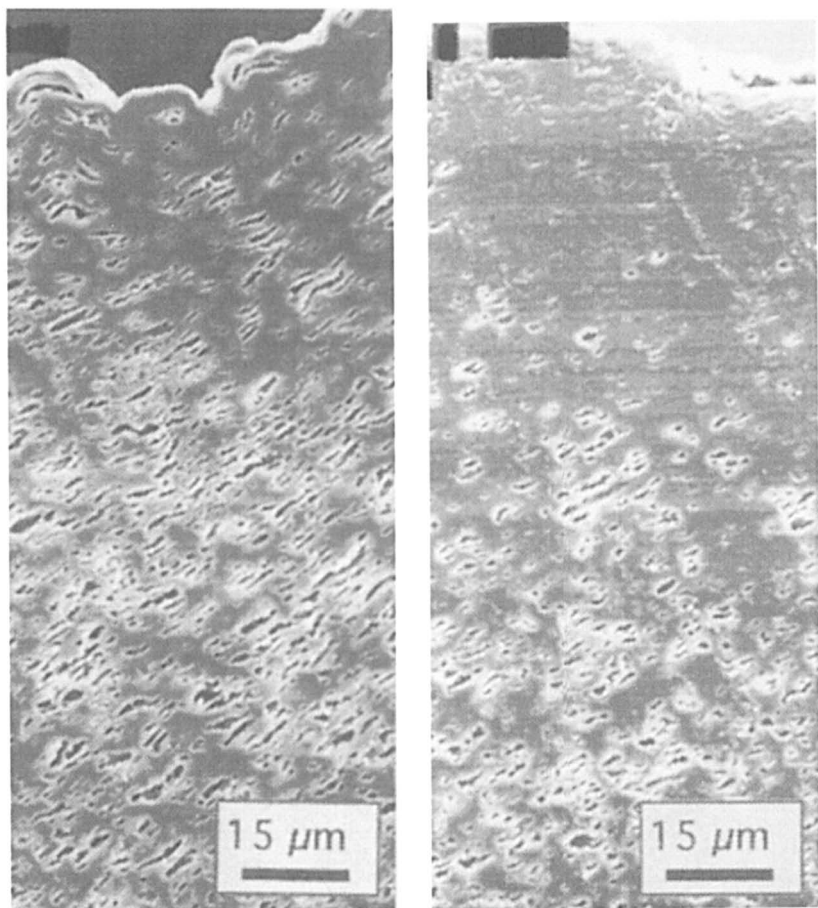


A



B

Figure 11. Structures of the fracture zone at different strainrates: A, 0.0275 s⁻¹; B, 0.275 s⁻¹; C, 2.75 s⁻¹; D, 22 s⁻¹. Reproduced with permission from reference 12.



C

D

Figure 11. *Continued.*

References

1. Van der Wal, A; Mulder, J.J.; Thijs, H.A.; Gaymans R.J., *Polymer* **1998**, *39*, 5467.
2. Gali, P.; Haylock, J.C., *Macromol. Chem. Macromol Symp.*, **1992**, *63*, 19.
3. Ramsteiner, F. *Polymer*, **1979**, *20*, 839.
4. Karger-Kocsis, J., *Polypropylene structure and properties*, Chapman Hall, London, Vol 2, 1995.
5. Chou, C.J.; K. Vijayan, K.; Kirby, D.; Hiltner, A.; and Baer, E., *J. Mat. Sci.* **1988**, *23*, 2521.
6. Greco, R.; Mancarella, C.; Martuscelli, E.; Ragosta, G.; Jinghua, J., *Polymer* **1987**, *28*, 1929.
7. Jang, B.Z.; Uhlmann, R.D.; Vander Sande, J.B., *J. Appl. Polym. Sci.* **1985**, *30*, 2485.
8. Michler, G.H., *Kunststoff-Mechanik: Morphologie, Deformations- und Bruchmechanismen*, Carl Hanser Verlag, Munich, 1992.
9. Ramsteiner, F. *Acta Polymerica*, **1991**, *42*, 584.
10. Inoue, T.; Suzuki, T., *J. Appl. Polym. Sci.* **1996**, *59*, 1443.
11. Van der Wal, A.; Mulder, J.J.; Oderkerk, J.; Gaymans, R.J., *Polymer*, **1998**, *39*, 6781.
12. Van der Wal, A.; Nijhof, R.; Gaymans, R.J., *Polymer*, **1999**, *40*, 6031.
13. Van der Wal, A.; Gaymans, R.J., *Polymer*, **1999**, *40*, 6045.
14. Bucknall, C.B., *Adv. Polym. Sci.*, **1978**, *27*, 121.
15. Donald, A.M.; Kramer, E.J., *J. Mat. Sci.*, **1982**, *17*, 1765.
16. Ramsteiner, F.; Heckmann, W., *Polym. Commun.* **1985**, *26*, 199.
17. Yee A.F.; Pearson, R.A., *J. Mat. Sci.*, **1986**, *21*, 2462.
18. Borggreve, R.J.M.; Gaymans, R.J.; Schuijjer, J., *Polymer*, **1989**, *30*, 71.
19. Dijkstra, K.; van der Wal, A.; Gaymans, R.J., *J. Mat. Sci.*, **1994**, *29*, 3489.
20. Dijkstra, K.; ten Bolsher, G.H., *J. Mat. Sci.*, **1994**, *29*, 4286.
21. Lazzeri, A.; Bucknall, C.B., *Polymer*, **1995**, *36*, 2895.
22. Van der Wal, A.; Verheul, A.J.J.; Gaymans, R.J., *Polymer*, **1999**, *40*, 6057.
23. Dijkstra, K.; Gaymans, R.J., *J. Mat. Sci.*, **1994**, *29*, 323.
24. Janik, H.; Gaymans, R.J.; Dijkstra, K., *Polymer*, **1995**, *36*, 4203.